CEAI, Vol. 6, No. 4, pp. 3-12, 2004 Printed in Romania

ROBUST CONTROL OF AN AUTONOMOUS WIND POWER SYSTEM

Nicolas Antonio CUTULULIS, Emil CEANGA

"Dunărea de Jos" University of Galați
Advanced Control Systems Research Center
111, Domnească, 800201-Galați, Romania

Abstract: *The paper deals with the robust control of wind power systems that uses a variable speed fixed pitch horizontal axis wind turbine (HAWT), driving a permanent magnet synchronous generator (PMSG) connected to a isolated local grid. In such wind power systems, the control problem consists in maximizing the energy captured from the wind for varying wind speeds. The paper focuses on the HAWT – PMSG power system modelling and dynamical analysis of the linearized system in various operating points on the characteristic of optimal regimes. This analysis revealed that the system is resonant and the natural frequency as well as the damping factor of the complex conjugated pole pair varies significantly along the operating point. In those conditions, the Quantitative Feedback Theory (QFT) method was used to design a control system for the autonomous wind power system. The resulted robust control structure is validated by numerical simulation.*

Keywords**:** *Robust control; QFT; Windmills; Autonomous systems; Permanent magnet generators.*

1. INTRODUCTION

Wind energy is the most important among the renewable power sources, due to the increased growth rate of the installed production capacities as a direct result of energy sustainable development strategy. Wind power systems are *grid connected* or *autonomous*. Grid-connected wind power systems are based on a "mature" technology, representing up to 10-15% of the total electrical energy production in some European countries [6]. During the last years, the use of the multipole permanent magnet synchronous generators (PMSG) is more and more common in wind power systems technology, having the main advantage of direct coupling to the wind turbine rotor, resulting in an important simplification of the mechanical system. [2], [5], [7].

The autonomous wind power systems are isolated power systems supplying local communities. In order to assure an uninterrupted energy supply, there are also other electrical energy sources: diesel generators, batteries and/or photovoltaic panels. A wind power system along with any of those sources (standard or renewable) form the so-called Hybrid Wind Power Systems (HWPS).

The main problem regarding wind power systems is the major discrepancy between the irregular character of the primary source (wind speed is a random, strongly non-stationary process, with turbulence and extreme variations, e.g. gusts) and the extremely exigent regulation demands regarding the electrical energy parameters (frequency, voltage, etc.). Thus, the wind energy conversion, at the parameters imposed by the energy market and the technical standards, is not possible without the essential contribution of automatic control.

The design of a control structure for a power system is not a trivial task, due to the parameters uncertainty and the highly nonlinear systems model.

Various robust control structures for grid connected wind power systems can be found in literature: sliding mode control [10], gain scheduling techniques [16], intelligent control [17].

An approach to the design of a robust controller can be based on the Quantitative Feedback Theory (QFT) method, which is widely used in robust controller design for nonlinear systems with parameters uncertainty: flight control systems [12], elastic mechanic positioning systems, biotechnologies [11], hydraulic systems [9], etc. Recently, a QFT pitch control structure for a grid-connected wind power system was presented in [13].

The problems presented in the paper regarding the control of the HWPS, are sensibly more complex compared to grid-connected wind power systems. The paper deals with a wind power systems that uses a variable speed fixed pitch horizontal axis wind turbine (HAWT), driving a PMSG connected to the local grid through power electronics, as shown in Figure 1.

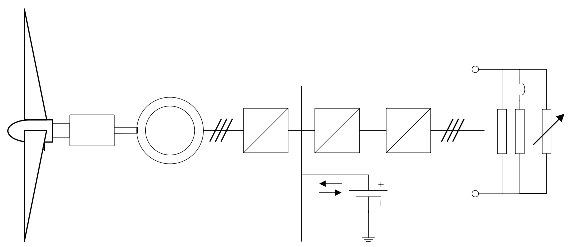

Fig. 1. The HAWT – PMSG power system

In such variable speed wind power systems, the control problem consists mainly in maximizing the energy captured from the wind for varying wind speeds.

The contributions presented in the paper concern the HAWT – PMSG power system modelling, dynamical analysis and designing of a robust controller using the QFT method.

The paper is structured as follows: the HAWT – PMSG power system modelling and dynamical analysis are presented in Section 2; the robust controller step by step design using the QFT method is presented in Section 3; Section 4 presents the numerical simulations conducted in order to validate the proposed robust controller. Finally, some concluding remarks end this paper.

2. SYSTEM MODELLING AND DYNAMICAL ANALYSIS

2.1. *Wind turbine mode*

The kinetic energy of the moving air masses (wind) is captured by the turbine and transformed into mechanical energy. If the wind energy is fully captured by the turbine rotor, the total power would be $P_t = 0.5 \cdot \pi \cdot \rho \cdot a \cdot v^3$, where ρ is the air density, a is the section area of the wind turbine and v is the wind speed. In reality the wind turbine harvest from the wind a mechanical power, P_w, smaller than the total power, P_t, due to the non-zero wind speed behind the rotor. According to Rankine – Froude theory, the expressions of P_w is obtained as [14]:

$$P_v = \frac{1}{2} \cdot \rho \cdot a \cdot v^3 \cdot C_p \tag{1}$$

where C_p is the power coefficient defining the aerodynamic efficiency of the wind turbine rotor. This is a function of the tip speed ratio, λ, defined as the ratio between the peripheral speed of the blades and the wind speed:

$$\lambda = \frac{R \cdot \Omega}{v} \tag{2}$$

where Ω is the rotational speed of the blades (the rotational speed of the low-speed shaft) and R is the blade radius.

The typical performance curve for a horizontal axis wind turbine is given in Figure 2. It presents a maximum for a well-determined tip speed, denoted by λ_{opt}.

The power characteristics for different wind speeds are given in Figure 3. For every wind speed they have a maximum. All these maxima determine a so-called *Optimal Regimes Characteristic* (ORC), as shown in Figure 3.

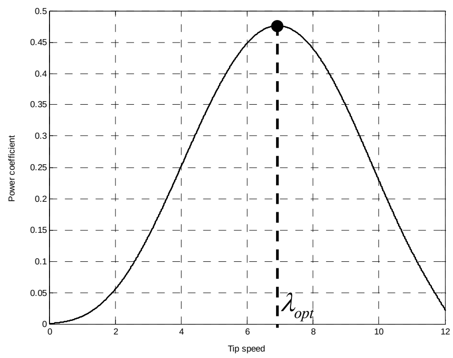

Fig.2. Power coefficient versus tip speed

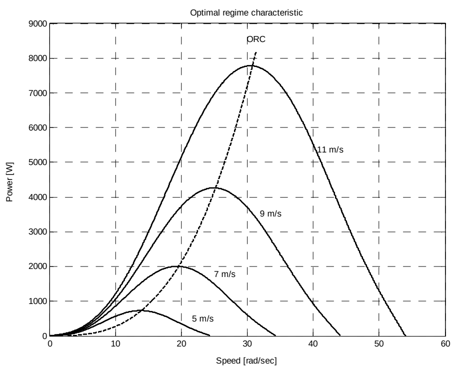

Fig.3. The optimal regime characteristics

The wind turbine provides the shaft's mechanical torque, according to the wind torque expression:

$$T_{\mathrm{w}} = 0.5 \cdot \rho \cdot \pi \cdot C_{\mathrm{T}}(\lambda) \cdot R^3 \cdot v^2 \tag{3}$$

where $C_{\mathrm{T}}(\lambda)$ is the torque coefficient, defined by:

$$C_{\mathrm{T}}(\lambda) = C_{\mathrm{p}}(\lambda) / \lambda \tag{4}$$

The torque coefficient is a designed parameter and the manufacturers of the wind turbine usually provide it. For the wind turbine considered in this paper, the torque coefficient is modelled as a 6th order polynomial regression [8]:

$$C_{\mathrm{T}}(\lambda) = a_0 + a_1\lambda + a_2\lambda^2 + a_3\lambda^3 + a_4\lambda^4 + a_5\lambda^5 + a_6\lambda^6 \tag{5}$$

with $a_{\mathrm{i}}, i = \overline{0,6}$ given in the Appendix. The torque coefficient described by Eq. (5) is plotted in Figure 4.

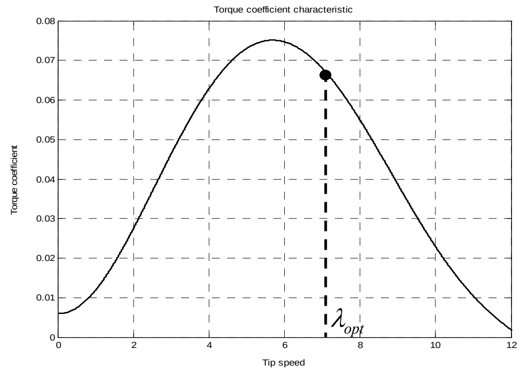

Fig.4. The torque coefficient versus tip speed

The operating point corresponding to optimal tip speed $(\lambda_{opt} = 7)$ lies on the descending portion of the torque coefficient, as it can be seen in Figure 4.

The gearbox is considered to be rigid and without dynamic, with a gear ratio $i = 10$.

2.2. *PMSG model*

The PMSG is modelled in the d-q frame, discarding the zero component. The state space systems model is:

$$\begin{aligned}
u_{\mathrm{d}} &= -R_{\mathrm{R}} i_{\mathrm{d}} - L_{\mathrm{d}} \frac{\mathrm{d}i_{\mathrm{d}}}{\mathrm{dt}} + pL_{\mathrm{q}}\omega i_{\mathrm{q}} \\
u_{\mathrm{q}} &= -R_{\mathrm{R}} i_{\mathrm{q}} - L_{\mathrm{q}} \frac{\mathrm{d}i_{\mathrm{q}}}{\mathrm{dt}} - p\left(L_{\mathrm{d}} i_{\mathrm{d}} - \Phi_{\mathrm{m}}\right)\omega \\
J\frac{\mathrm{d}\omega}{\mathrm{dt}} &= T_{\mathrm{w}} - p\left[\Phi_{\mathrm{m}} i_{\mathrm{q}} - \left(L_{\mathrm{d}} - L_{\mathrm{q}}\right) i_{\mathrm{d}} i_{\mathrm{q}}\right]
\end{aligned} \tag{6}$$

where R_{R} - the rotor resistance, p - the pole pair number, $L_{\mathrm{d}}, L_{\mathrm{q}}$ - the rotor inductances in the d-q axes, u_{d} and u_{q} - the d-q axes voltages, J - the moment of inertia and Φ_{m} - the permanent magnet flux. In grid-connected wind power systems the d-q axes voltages, u_{d} and u_{q}, are input variables. In autonomous wind power systems, when the PMSG is connected to a local grid, u_{d} and u_{q} become output variables. In this case the PMSG's model should also include the local grid equations. The voltages on the d-q axes, described by the local grid equations, are:

$$\begin{bmatrix} u_{\mathrm{d}} \\ u_{\mathrm{q}} \end{bmatrix} = R_{\mathrm{s}} \cdot \begin{bmatrix} i_{\mathrm{d}} \\ i_{\mathrm{q}} \end{bmatrix} + L_{\mathrm{s}} \frac{\mathrm{d}}{\mathrm{dt}} \cdot \begin{bmatrix} i_{\mathrm{d}} \\ i_{\mathrm{q}} \end{bmatrix} + X \cdot \begin{bmatrix} i_{\mathrm{d}} \\ i_{\mathrm{q}} \end{bmatrix} \tag{7}$$

where

$$X = T^{-1} \cdot \frac{\mathrm{d}T^{-1}}{\mathrm{d}t} = \begin{bmatrix} o & \omega L_s \\ -\omega L_s & 0 \end{bmatrix} \qquad (8)$$

with R_s - the load resistance, L_s - the load inductance and T - the Park transformation matrix [15].

Using (7) and (8), the model (6) can be written in the form:

$$\begin{aligned} &(L_d+L_s)\frac{\mathrm{d}i_d}{\mathrm{d}t} = -(R+R_s)i_d + p(L_q+L_s)i_q\omega \\ &(L_q+L_s)\frac{\mathrm{d}i_q}{\mathrm{d}t} = -(R+R_s)i_q - p(L_d+L_s)i_d\omega + p\Phi_m\omega \qquad (9) \\ &J\frac{\mathrm{d}\Omega}{\mathrm{d}t} = T_w - T_{em} = T_w - p\left[(L_d-L_q)i_d i_q - \Phi_m i_q\right] \end{aligned}$$

The dynamic of the power electronics being significantly more rapid than the HAWT – PMSG dynamic, was neglected. Thus, the input variable R_s represents the equivalent load resistance at generator's terminals.

2.3. *Dynamical analysis of the wind power system*

In order to maximize the power extracted from the wind, the tip speed ratio should be kept around its optimal value, λ_{opt}. Though, the wind power systems is controlled in close loop, in such way that the shaft speed tracks the speed reference Ω^{ref}, calculated from (2), according to the measured wind speed v :

$$\Omega^{ref} = \frac{\lambda_{opt}}{R} v \qquad (10)$$

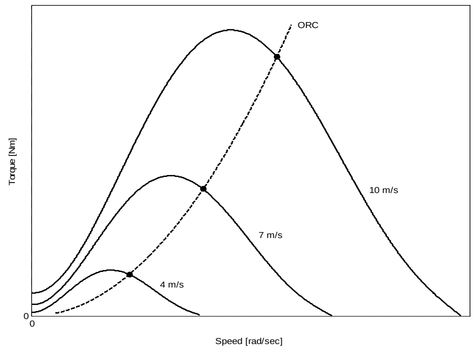

Fig.5. The operating points

The nonlinear HAWT – PMSG power system model (9) was linearized in three operating points defined by the wind speed v (4; 7 and 10 m/s) and the load resistance R_s (14.6; 25.9; 38 ohm) in such manner that they lie on the ORC. The operating points are presented in Fig. 5.

The pole distribution and step response of the HAWT – PMSG system, linearized in the above-mentioned operating points, are shown in Figure 6 and 7, respectively.

The linearized HAWT- PMSG system has a pole distribution strongly dependent on the operating point. When the operating points are considered on the ORC, the linearized HAWT – PMSG system is resonant, and the natural frequency, as well as the damping factor of the complex conjugated pole pair, varies significantly along the ORC.

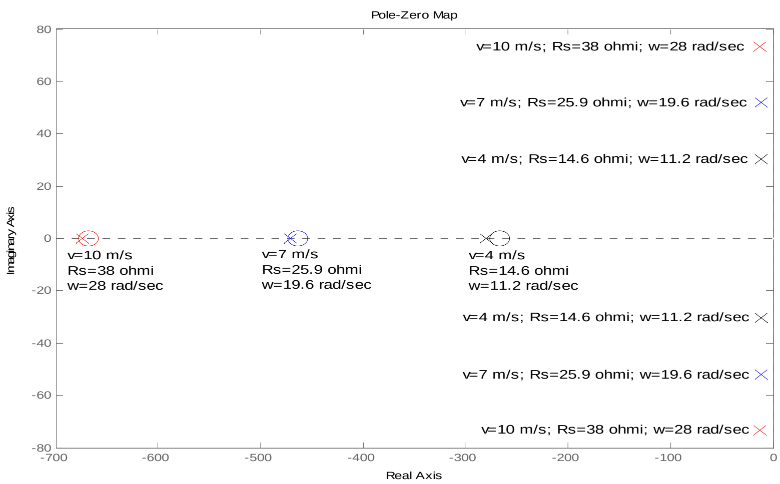

Fig.6. The pole distribution

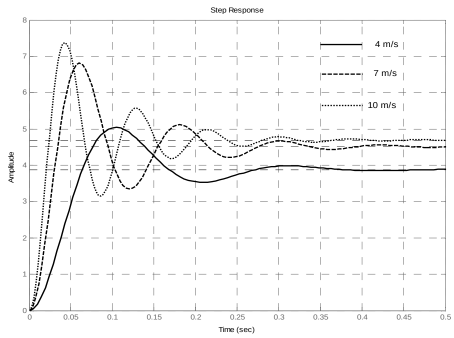

Fig.7. The linearised HAWT – PMSG step response

3. STEP BY STEP CONTROLLER DESIGN

The QFT design technique is based on the frequency domain shaping of the *open – loop* transfer function [4]. The uncertainties in the plant gain and phase are represented as a template on the Nichols chart and used to define regions in the frequency domain where the open – loop frequency response must lie in order to satisfy the performance and stability specifications.

The QFT design method employs a two-degree freedom control structure, using a compensator $C(s)$ and a prefilter $F(s)$, as shown in Figure 8.

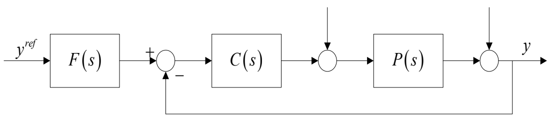

Fig.8. Two degree freedom structure

The tracking control structure synthesis – according to the QFT design method steps [12] – is presented next. The tracking control loop aims to maintain the operating points of the autonomous wind power system on the ORC.

1. *System formulation*. The HAWT – PMSG power system model is represented by a series of linear time invariant (LTI) transfer functions in various points of the operating range. The operating range is determined by the wind speed. We consider the bounds of the operating regime defined by the starting wind speed ($v_s = 3\,\text{m/s}$) and the nominal wind speed ($v_n = 10\,\text{m/s}$). The nonlinear HAWT – PMSG power system model (9) was linearized in the above defined 3 operating points (Figure 5).

After neglecting the irrelevant time constant, the resulting transfer function describing the system proprieties around the three operating points is:

$$H_p(s) = \frac{k}{T^2 \cdot s^2 + 2\zeta T \cdot s + 1} \tag{11}$$

The operating points and parameters values are presented in Table 1.

Table 1. Operating points

Wind speed	Load resistance	k	T	ζ
4 m/s	14,6 Ω	3,88	0,0751	0,6147
7 m/s	25,9 Ω	4,52	0,0456	0,2440
10 m/s	38 Ω	4,69	0,0326	0,1512

In order to facilitate the QFT design method, the linear LTI model (11) is approximated by:

$$H_p(s) = \frac{k}{T^2 \cdot s^2 + 2\zeta T \cdot s + 1} \tag{12}$$

where $\zeta = 0.8$ is a constant. The Bode characteristics of the LTI wind power system models defined by (11) are bounded by the transfer function (12), as shown in Figure 9. The variation ranges for k and T in Eq. (11) are:

$$k = [3{,}5 \div 16];\; T = [0.015 \div 0.085] \tag{13}$$

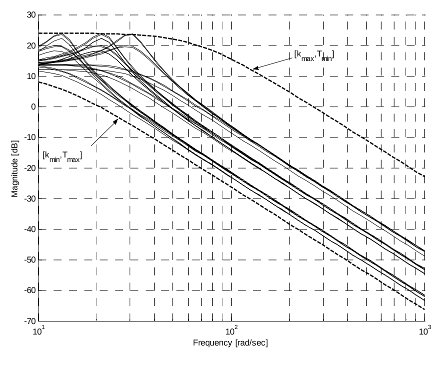

Fig.9. Bounding of the LTI power system models Bode characteristic

2. *Performance design specifications*. The performance specifications impose the desired dynamic and steady-state performance of the closed-loop system. The tracking specification defines the acceptable variations domain of the closed loop tracking response due to parameter uncertainty and disturbances and it is usually defined in the time domain:

$$y_L(t) \le y(t) \le y_U(t) \tag{14}$$

where $y(t)$ denotes the system tracking step response; $y_L(t)$ and $y_U(t)$ denote the lower and respectively the upper tracking bounds for step response. Since QFT is a frequency-domain design method, the time-domain tracking specifications must be transformed into the frequency domain.

For the considered HAWT – PMSG power system the tracking performance is defined by the nominal transfer function:

$$H_T(s) = \frac{\omega_n^2}{s^2 + 2\zeta\omega_n s + \omega_n^2} \qquad (15)$$

where ω_n and ζ determine the nominal regime system performance. It was adopted: $\omega_n = 20$ and $\zeta = 0.9$.

The upper and lower tracking bounds are defined by:

$$H_{TU}(s) = \frac{\frac{\omega_0^2}{a}(s+a)}{s^2 + 2\zeta\omega_0 + \omega_0^2} \qquad (16)$$

$$H_{TL}(s) = \frac{a_1 \cdot a_2 \cdot a_3}{(s+a_1)(s+a_2)(s+a_3)}$$

where $a = 1.2\omega_n$; $a_1 = 0.5\omega_n$; $a_2 = 1.5\omega_n$ and $a_3 = 2\omega_n$.

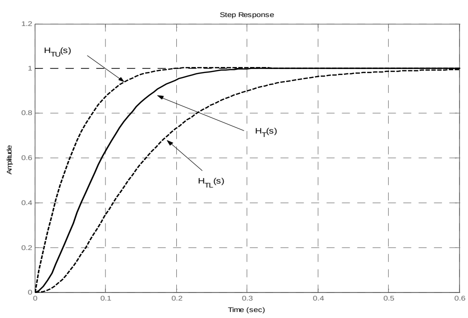

Fig.10. Tracking bounds step response

The tracking bounds in time domain (step response) and in frequency domain are presented in Fig. 10 and Fig.11, respectively.

The robust stability specification assures the closed loop stability, regardless of the plant parameters variation in the considered uncertainty region and it is defined as follows:

$$\left| \frac{C(j\omega)P(j\omega)}{1 + C(j\omega)P(j\omega)} \right| \le \alpha_B \qquad (17)$$

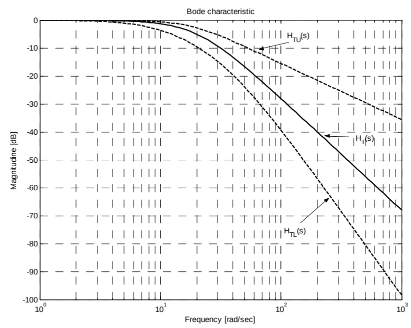

Fig.11. Bode characteristic of the tracking bounds

Usually, $\alpha_B < 2\text{dB}$ so $\alpha_B = 1.2 \cong 1.6\text{dB}$ is chosen.

3. *Templates and computation of bounds*. The trial frequency array used in the QFT design method is:

$$\omega = [1 \quad 5 \quad 10 \quad 20 \quad 40 \quad 100] \text{ rad/sec} \qquad (18)$$

The plant templates at these frequency points and the variation ranges (13) for *k* and *T* are computed with the QFT toolbox in Matlab® and presented in Figure 12.

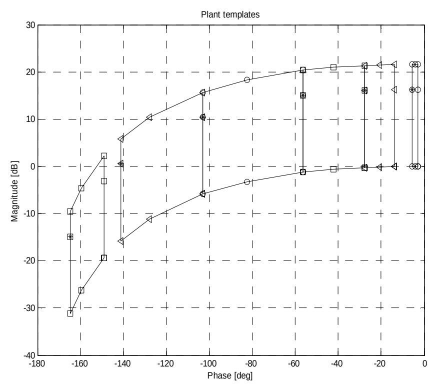

Fig.12. Plant templates

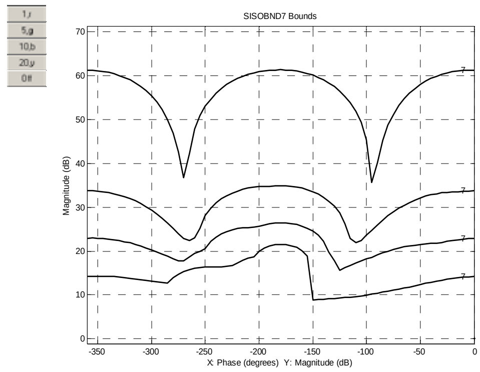

Fig.13. Tracking bounds

The tracking and the robust stability margin bounds in the Nichols plane are computed with the QFT toolbox in Matlab® on the basis of the performance specifications and the plant templates.

The tracking bounds are presented in Figure 13. The robust stability margin bounds, also computed with the QFT toolbox in Matlab®, are presented in Fig. 14.

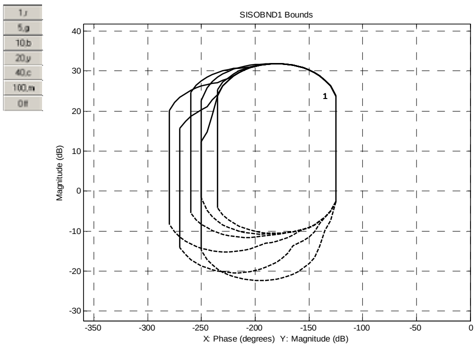

Fig.14. Robust stability margin bounds

4. *Loop shaping controller design*. At this point, the intersection between tracking response and robust stability bounds is computed and plotted along with the open loop transfer function $L(j\omega)=C(j\omega)\cdot P(j\omega)$. The open loop frequency response must lie on or above the bounds at each of the trial frequency (Figure 15).

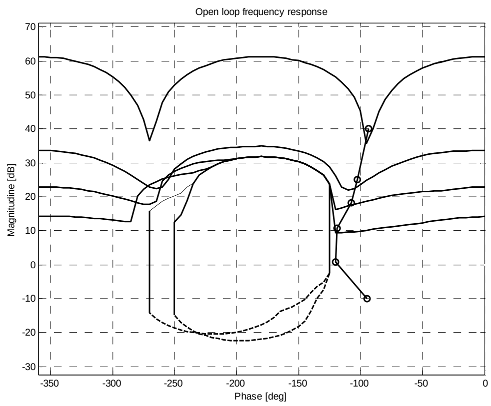

Fig.15. Open loop frequency response with controller

If this condition is satisfied for the considered nominal plant, then the condition is satisfied for all plants described by the uncertainty [4].

The controller $C(s)$ has an initial expression and the design is performed in a very transparent and interactive manner by adding gains or dynamic elements to the nominal plant frequency response in order to change the shape of the open loop transfer function in such manner that the boundaries are satisfied at any trial frequencies. After performing those adjustments, the final open loop frequency response obtained for the HAWT – PMSG power system is presented in Figure 15. The controller's transfer function expression, obtained with this procedure, is:

$$C(s)=\frac{6.84(s+62.5)(s+10.06)(s+9.93)}{s(s+1265)(s+5.24)} \tag{19}$$

5. *Prefilter design.* The loop shaping of the open loop frequency response ensures that the closed loop response fulfils the stability performances in the frequency domain. The prefilter $F(s)$ (Figure 8) is designed to shape the output of the system to satisfy the tracking specifications. The prefilter shaping is carried out using a Bode characteristic and it is done in the same interactive manner. The prefilter transfer function thus obtained is:

$$F(s)=\frac{5478.55}{(s+343.7)(s+15.94)} \tag{20}$$

6. *Verification of stability and robust tracking conditions*. Firstly, the robust stability specification (17) of the closed loop system is verified. The closed loop system Bode characteristic is presented in Figure 16 and it can be seen that the robust stability performance is satisfied (for $\alpha_{\mathrm{B}}=1.6\,\mathrm{dB}$).

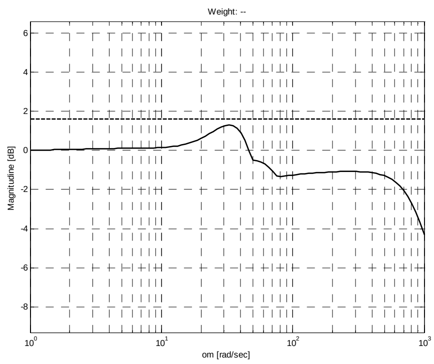

Fig. 16. The robust stability condition

In order to verify the tracking performances, the closed loop frequency response of the HAWT – PMSG power system without the prefilter is determined (Figure 17).

The closed loop response without prefilter satisfies the stability performances in the frequency domain – the response bandwidth (solid line) is smaller than the bandwidth defined by the upper and lower limit stability specifications (dotted line) – but the robust tracking specification are not satisfied. The closed loop response with the designed prefilter is presented in Figure 18. We observe that after inserting the designed prefilter, the close loop response satisfies both stability and robust tracking performances, thus a successful design is achieved.

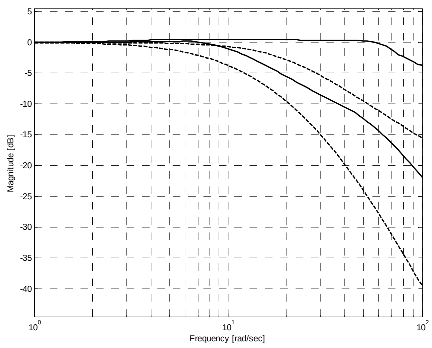

Fig.17. Close loop response without prefilter

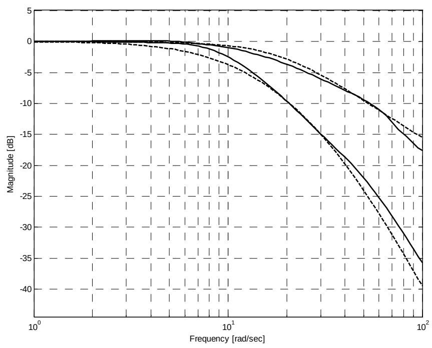

Fig.18. Close loop response with prefilter

4. NUMERICAL SIMULATION RESULTS

The robust control structure designed using the QFT design method was numerically simulated in Matlab/SIMULINK®. The HAWT – PMSG power system was implemented using the nonlinear model presented in (9). The robust tracking control block scheme is presented in Figure 19.

The aim of the robust control scheme is to maximize the energy captured from wind, for varying wind conditions, thus maintaining the tip speed at optimal value $\left(\lambda_{\text{opt}} = 7\right)$. The speed reference Ω^{ref} is calculated based on the measured v, according to (10).

The first numerical simulation scheme conducted to validate the robust controller used as the input signal a determinist speed reference covering in steps the operating range corresponding to wind speeds from $v = 3$ m/s to $v = 11$ m/s. The simulation results are presented in Figure 20.

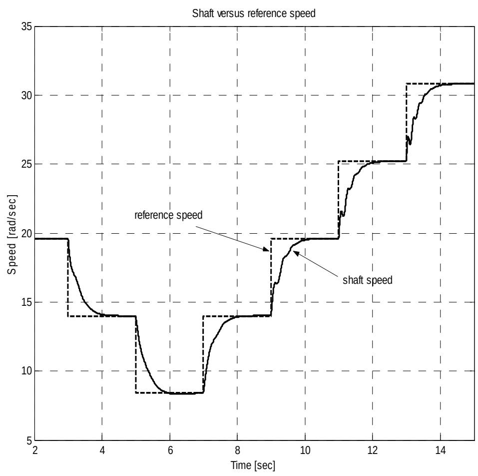

Fig.20. Shaft speed versus reference speed

The signal presented in Figure 21 represents a realistic wind profile, modelled as a non-stationary stochastic process in [3] and used as the input to the simulation.

The wind profile covers a speed range between $4 \div 11$m/s, which represents the range between wind turbine starting speed and nominal speed. This is the speed range that covers most of the wind turbine's operating time.

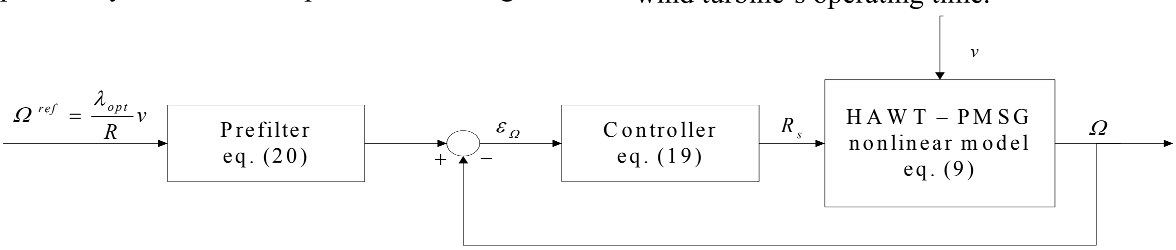

Fig.19. – PMSG power system robust control bloc scheme

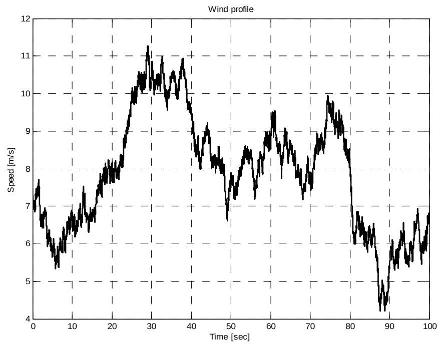

Fig.21. The wind profile

The effectiveness of the robust tracking control scheme can be seen in Figure 22. The controller ensures maximum energy caption from wind, for wind speed varying from 4 to 11 m/s. The tip speed is maintained around its optimal value $\left(\lambda_{opt} = 7\right)$ with some minor dynamical errors due to the turbulence component.

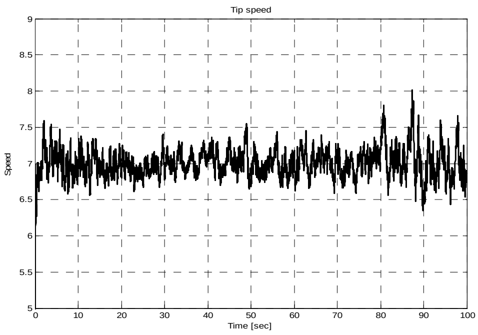

Fig.22. Tip speed evolution

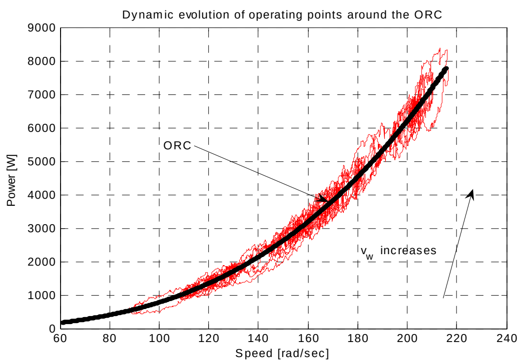

Fig.23. Dymanic evolution of operating point around the ORC

The robust tracking control scheme maintains the operating point around the ORC for wind speeds varying from 4 to 11 m/s, thus ensures the maximum energy conversion.

5. CONCLUDING REMARKS

The control of autonomous wind power systems is a very difficult task. The analyzed autonomous wind power system uses a permanent magnet synchronous generator, along with alternative electrical (batteries) and photovoltaic source, representing a typical for supplying small isolated grids.

A first contribution in the paper is the HAWT – PMSG power system's nonlinear model. The analysis of the linearized model in various operating points on the ORC revealed that the system is resonant and the natural frequency as well as the damping factor of the complex conjugated pole pair varies significantly along the operating point. In those conditions, the QFT method was used to design a control system for the autonomous wind power system. The numerical simulations conducted in Matlab/SIMULINK® proved the effectiveness of the proposed control structure.

6. REFERENCES

[1] Breslin, S. G., Grimble, M. J. - "Robust Flight Control using Quantitative Feedback Theory: Preliminary Design Studies". Technical Report, ICC/123/96, Industrial Control Centre, University of Strathclyde, 1996.

[2] Chalmers, B. J., Wu, W., Spooner, E. - "An Axial-Flux Permanent-Magnet Generator for a Gearless Wind Energy System". IEEE Trans. on Energy Conversion, Vol. 14, No. 2, pp. 251 – 257, 1999.

[3] Cutululis, N. A., Munteanu, I., Ceanga, E., Culea, M.,. - "Optimal Control Structure for Variable Speed Wind Power Systems". 11-th National Conference on Electric Drives, Proceedings CNAE-2002, Galati, Romania, pp. 121 – 128, 2002

[4] Horowitz, I.M. - "Quantitative Feedback Design Theory". Vol.1, QFT Publications, Colorado. 1993

[5] Kladas, A. G., Papadopoulos, M. P. Tegopoulos, M. P. - "Multipole permanent magnet generator design for gearless wind power applications", Proceedings of the International Conference on Electrical Machines ICEM'98, Istanbul, Turkey pp. 2055-2059, 1998.

[6] Ackermann, T. and L. Söder, *Wind energy technology and current status: a review*,

Renewable and Sustainable Energy Reviews, 4, Pergamon Press, pp. 315-374.
[7] Lampola, P. - “Electromagnetic Design of an Unconventional Directly Driven Permanent-Magnet Wind Generator”, Proceedings of the International Conference on Electrical Machines ICEM'98, Istanbul, Turkey, pp. 1705-1710, 1998.
[8] Nichita, C.- “Etude et développement de structures et lois de commande numériques pour la réalisation d’un simulateur de turbine éolienne de 3 kW“, Thèse de Doctorat, Université du Havre, France, 1995
[9] Niksefat, N., Sepehri, N. - “Design and Experimental Evaluation of a Robust Force Controller for an Electro – Hydraulic Actuator via Quantitative Feedback Theory“, Control Engineering Practice, Vol. 8, pp.1335-1345, 2000.
[10] De Battista, H., R.J. Mantz and C.F. Christiansen, *Dynamical Sliding Mode Power Control of Wind Driven Induction Generators*, IEEE Transactions on Energy Conversion, Volume 15, No. 4, December 2000, pp. 451-457.
[11] Skogestad, S., Morari, M., Doyle, J. C. “Robust control of ill conditioned plants; high purity distillation”. IEEE Transactions on Automatic Control, Vol. 33, pp. 1092-1105, 1989
[12] Wu, S. F., Grimble, M. J., Breslin, S. G. - “Introduction to Quantitative Feedback Theory for lateral robust flight control systems design”, Control Engineering Practice, Vol. 6, pp. 805-828, 1998.
[13] Torres, E., Garcia-Sanz, M. – “Experimental Results of the Variable Speed, Direct Drive Multipole Synchronous Wind Turbine TWT1650”, Wind Energy, Vol. **7**, pp.109–118, 2004.
[14] Burton, T., Sharpe, D. Jenkins, N., Bossanyi, E. - “Wind Energy Handbook”, John Wiley & Sons, 2001.
[15] Leomhard, W. – “Control of Electrical Drives”, Springer-Verlag, New York, 1986.
[16] Bianchi, F. D., Mantz, R. J., Christiansen, C. F. *Gain scheduling control of variable-speed wind energy conversion systems using quasi-LPV models*. Control Engineering Practice, Volume 13, Issue 2, pp. 247-255
[17] Simoes, M.G., B.K. Bose and R.J. Spiegel, *Fuzzy Logic Based Intelligent Control of a Variable Speed Cage Machine Wind Generation System*, IEEE Transactions on Power Electronics, Volume 12, No. 1, January 1997, pp 87-95.

7. APPENDIX

PMSG parameters:

$R_{\mathrm{R}} = 3,3\,\Omega$;
$L_{\mathrm{d}} = L_{\mathrm{q}} = 0.04156$ H;
$J = 0.042\,\mathrm{kgm}^2$;
$\Phi_{\mathrm{m}} = 0.4382\,\mathrm{Wb}$;
$p = 3$;

Wind turbine parameters:

$\rho = 1.25\,\mathrm{kg/m}^3$;
$R_{\mathrm{t}} = 2.5\,\mathrm{m}$;
$J_{\mathrm{T}} = 0.005\,\mathrm{kgm}^2$
$a_0 = 0.0061$; $a_1 = -0.0013$; $a_2 = 0.0081$;
$a_3 = -9.7477.10^{-4}$; $a_4 = -6.5416 \cdot 10^{-5}$;
$a_5 = 1.3027 \cdot 10^{-5}$; $a_6 = -4.54 \cdot 10^{-7}$.